

Experimental studies of flow through single gauzes

C.-C. Su and C.-C. Huang

Mechanical Engineering Department, National Taiwan University, Taipei, Taiwan, Republic of China

This article describes the experimental studies on the effect of flow Mach number and Reynolds number, the open area ratio of the gauze, and the ratio of specific heats of the fluid on the pressure drop of the flow through wire screens. The gauzes tested were of ten different values of open area ratio. Air and helium were used as the test fluid. The results show that the pressure loss coefficient increases with Mach number and that the increase is sharp at choking. In the incompressible flow regime, the pressure loss coefficient decreases with increasing Reynolds number and open area ratio. However, the effect of the ratio of specific heats is negligible. Empirical relations for the pressure loss coefficient were derived based on these test results.

Keywords: pressure drop; single gauze; open area ratio; compressible flow

Introduction

Single gauze has been used as a filter, to control turbulence, and to create or eliminate large-scale velocity or pressure nonuniformities. Due to the high ratio between their surface area and volume, finely woven gauzes are also suitable as the packing material of the regenerator of the Stirling cycle machine. Unfortunately, no studies seem to have shed light on how the flow characteristics of single gauze combine to produce the properties of the matrix of stacked gauzes used as regenerators. A detailed study of the flow through single gauzes is therefore necessary.

The first experimental work on the pressure drop of the flow through single gauzes can be traced back to Adler.¹ The variations of the pressure loss coefficient of the flow, f (defined as the pressure drop across the gauze divided by the upstream kinetic energy), versus the upstream Mach number, M , were plotted for different open area ratios of the gauze, σ . Later on, the Reynolds number, Re , was pointed out to be another governing factor of the pressure drop characteristics.²⁻⁴ Pinker and Herbert⁵ have tried to separate the individual effect of M , Re , and σ on f . However, Roach^{6,7} pointed out that the influence of Re and M appeared to have been confused. The studies were thus concentrated on the case of incompressible flow. Su⁸ also pointed out that Pinker and Herbert did not successfully separate the effects of these three governing factors, since they used the irrelevant upstream Reynolds number. Furthermore, based on the flow model of a one-dimensional (1-D) core outside the boundary layer developed along the wire surface, Su⁸ found that the specific heat ratio, γ , of the fluid may also be an influencing factor. The deficiency in assuming that the core is 1-D was corrected later by Su, Hsieh, and Chiu.⁹ The results also show that the pressure-drop characteristics are influenced by the four governing factors, namely, M , Re , σ , and γ . Although Su's work⁸ contains some experimental data of pressure drop across single gauzes, the range of σ investigated is quite narrow, i.e., from 0.365 to 0.379. The work still to be solved is thus the experimental verification of these simulations with a convincingly broad range of σ .

Address reprint requests to Dr. Su at the Mechanical Engineering Department, National Taiwan University, Taipei, Taiwan, R.O.C.

Received 24 October 1990; accepted 26 February 1991

Experimentation

Eighteen single gauzes were tested. The specifications of these gauzes are listed in Table 1. The material of these gauzes was stainless steel except for gauze A1, which was copper. The wire diameter and the aperture of the gauzes ranged from 0.036 to 0.16 mm and 0.05 to 0.63 mm, respectively. The open area ratio, σ , of the gauzes ranged from 0.31 to 0.64 and was divided into ten groups. Each group had the same value of σ , but might contain gauzes of different wire diameters and apertures, as shown in the table.

The test circuit for the investigation of the pressure drop across single gauzes is shown in Figure 1. Detailed description of the test system and the experimental procedure can be found in the work of Huang.¹⁰ The design working pressure of the system was 10 bar at room temperature. The test section shown was made of nylon 6/6. Single gauzes were clamped between the two gauze holders of the test section. Tappings

Table 1 Specifications of gauzes tested

Gauze	Aperture l , mm	Wire diameter d , mm	Mesh number m , inch ⁻¹	Open area ratio, σ
A1	0.14	0.11	100	
A2	0.14	0.11	101	0.31
A3	0.05	0.04	280	
B	0.071	0.05	210	0.34
C1	0.2	0.125	78	
C2	0.16	0.10	98	
C3	0.15	0.10	100	0.38
C4	0.08	0.05	200	
C5	0.062	0.04	250	
D1	0.066	0.036	250	
D2	0.064	0.036	255	0.41
E	0.18	0.09	94	0.44
F1	0.23	0.10	78	0.48
F2	0.09	0.04	195	
G	0.36	0.14	51	0.51
H	0.32	0.11	59	0.64
I	0.51	0.16	38	0.57
J	0.63	0.16	32	0.64

Note: The material was stainless steel, except for gauze A1, which was copper.

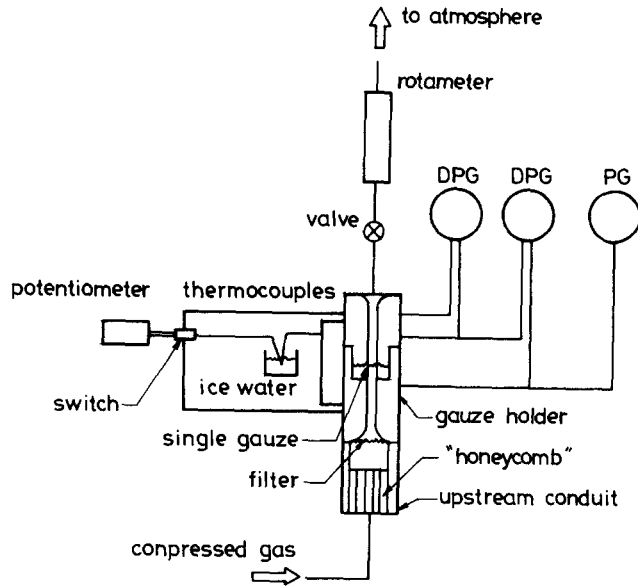


Figure 1 Schematic of the test system (DPG, differential pressure gauge; PG, pressure gauge)

were provided as shown for temperature and pressure measurements. The inside diameter of the assembly was 3.0 mm and that of the conduits at the upstream and downstream sides was 20 mm each. A filter consisting of six layers of gauze C5 of 250 mesh per inch was clamped between the upstream gauze holder and conduit to prevent foreign materials from entering the test section. This filter was cleaned each time the test gauze was changed. Since a pressure hump behind the single gauze had been observed by Pinker and Herbert,⁵ the downstream tapping for the pressure measurement was located 18 mm behind the single gauze to avoid misleading results. The entrance and the exit of the gauze holders were rounded for the purpose of reducing the turbulence induced by the abrupt change in flow area. In order to make the upstream flow uniform, the upstream conduit contained a ring designed according to the criteria suggested by Loehrke and Nagib.¹¹ This ring was 20 mm in length and was stacked with stainless steel tube of 0.63 mm OD and 0.33 mm ID.

Four pressure gauges were used in the test. Two of them were of differential type, while others were of absolute type. These gauges had been calibrated with water and mercury manometers. The maximum error in reading was within $\pm 2.0\%$ of the capacity of the gauges; therefore, no correction was taken in pressure readings. The arrangement of these pressure gauges is shown in Figure 1. The upstream pressure was monitored by the ordinary gauge, while the pressure difference across the

single gauze was monitored by the differential pressure gauge of 2 bar capacity. In addition, another differential pressure gauge was used to measure the pressure drop in the downstream conduit. The pressure immediately after the gauze could then be obtained through extrapolation using measured pressure drop in the downstream conduit. However, the pressure immediately before the gauze was estimated through measured upstream pressure and the correlation for the pressure drop of laminar flow in a circular duct. The distance between the upstream pressure tapping and the section where the single gauze was located was 9 mm, while that between the two tappings for the downstream differential pressure gauge was 12 mm. However, the first tapping behind the single gauze was 18 mm behind the gauze to avoid measuring the misleading pressure hump induced by the jet observed by Pinker and Herbert.⁵

The absolute temperature at the upstream side of the gauze, T_{up} , was measured with an ordinary thermocouple, while the temperature difference between the upstream and downstream sides was monitored with a differential thermocouple, as shown in Figure 1. Both thermocouples were of copper/constantan type and were calibrated beforehand.

Two rotameters were used to monitor the volume flow rate of the working fluid. Depending on the required flow rate for a given flow condition, these meters were used independently. The capacity of these meters was $3.3 \times 10^{-3} \text{ m}^3/\text{s}$ (200 liter/min) and $16.7 \times 10^{-3} \text{ m}^3/\text{s}$ (1000 liter/min). These rotameters were designed for measuring air flow rate. In the test with helium as the working fluid, the actual flow rate was estimated through the square root of the density ratio between air and helium.

Before the test, the single gauzes were cleaned with acetone in an ultrasonic cleaner. Compressed air and helium from a gas bottle were passed through the test section of the apparatus. Pressure, temperature, and volume flow rate were then read through the meters described above.

Results and discussion

Effect of the Mach number

Figure 2 shows the variation of the pressure loss coefficient, f , with upstream Mach number, M , for five values of open area ratio, σ . These values of σ cover the entire range of σ investigated. Results of other values of σ lie between those shown in this figure. Note that f is defined as the ratio between the difference in upstream and downstream pressures and the upstream kinetic energy of the fluid, i.e.,

$$f = \frac{P_{up} - P_{dn}}{(\rho u^2/2)_{up}} \quad (1)$$

Notation

d	Wire diameter
f	Pressure loss coefficient
l	Aperture
M	Upstream Mach number
M^*	Upstream choking Mach number
m	Mesh number
P	Pressure
Re	Reynolds number
T	Temperature
u	Velocity

Greek symbols

γ	Ratio of specific heats
ζ	$= \text{Re}/2000$
ρ	Density
σ	Open area ratio
σ_{sin}	Sinusoidal open area ratio (Equation (3))

Subscripts

dn	Downstream conditions
inc	Incompressible conditions
isen	Isentropic conditions
up	Upstream conditions

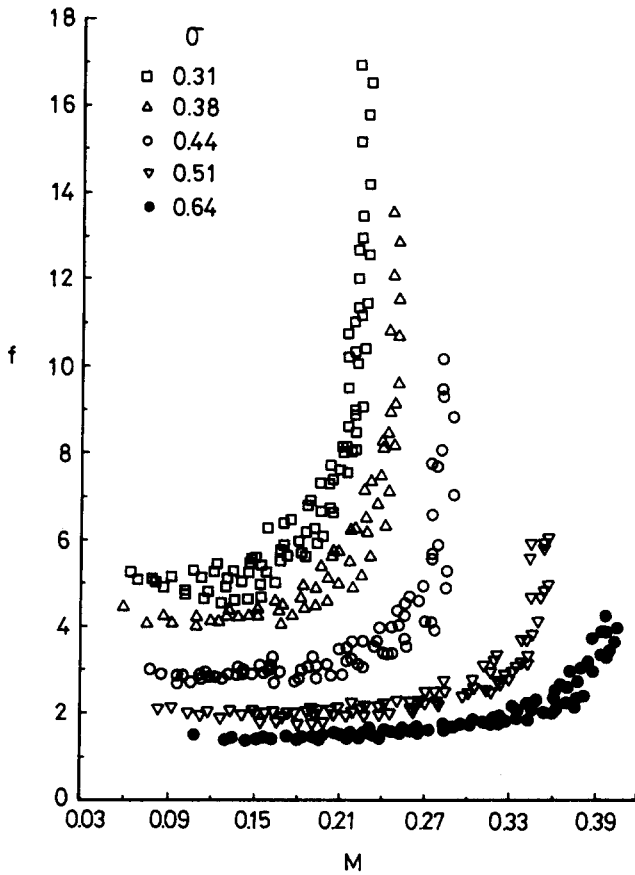


Figure 2 *f* versus *M* for different values of σ

and that σ is defined as

$$\sigma = 1 - \frac{\text{block area}}{\text{flow area}} = \left(\frac{l}{d+l} \right)^2 \quad (2)$$

It can be seen from Figure 2 that for each group of σ , f increases with M and the increase is sharp at some value of M , indicating that choking has occurred. The choking Mach number, M^* , was suggested by Adler¹ and Pinker and Herbert⁵ to be constant for a given σ . However, Figure 2 shows that M^* varies somewhat for each σ . In fact, the higher the Reynolds number, Re , is, the lower M^* tends to be. Nevertheless, the variation is within about 5% of M^* for each σ . The choking Mach number may therefore be taken as constant for each given value of σ .

Figure 3 shows M^* versus σ . The discrepancy in M^* between the present measured results and those predicted by the isentropic relationship between Mach number and free-flow area without considering the effect of the boundary layer is relatively small. Physically, there must be a boundary layer developing along the wire surface. However, the weaving of the wire may make the free-flow area different somewhat from that calculated using Equation 2. This weaving effect had been pointed out by Pinker and Herbert.⁵ Due to the high values of M^* , as shown in Figure 3, Pinker and Herbert suggested a sinusoidal open area ratio, σ_{sin} , defined as

$$\sigma_{sin} = 1 - \frac{2}{\pi^2} \left\{ (1 + 2g^2) \left(\frac{\pi}{2} - \cos^{-1} g \right) + 3g(1 - g^2)^{1/2} \right\} \quad (3)$$

where $g = \pi md/2$. By using σ_{sin} , the agreement between their test results and the isentropic choking Mach number, M_{isen}^* , is improved, as can be seen from Figure 3. However, if σ_{sin} were used, M^* of the present work would be much lower than M_{isen}^* , as shown in Figure 3. Since the results of Adler¹ also show that no adjustment in open area ratio is necessary, the results of the present work are considered more reliable.

The variation of f with M has the same tendency as those obtained by the above-mentioned earlier works. Based on the experimental results of the present work, an empirical relationship between f and M is thus derived as

$$f = f_{inc} \left(\frac{M^*}{M^* - M} \right)^{0.16} \quad (4)$$

The form of this expression is the same as that suggested by Pinker and Herbert,⁵ Su,⁸ and Su, Hsieh, and Chiu.⁹ The only distinction is that the value of the exponent of the expression is different for different works. The exponent in Equation 4 is 0.16, while those suggested by Pinker and Herbert,⁵ Su,⁸ and Su, Hsieh, and Chiu⁹ are 1/7, 1/5, and 0.176, respectively. The difference in the general variation of the curve is not great, as can be seen from Figure 4—in fact, more important is the difference in the value of f_{inc} , which is defined as f at $M=0$ and is obtained through the extrapolation of the measured values.

Figure 4 shows that for a given Re , the values of f of the present work are consistently lower than those of the experimental results of Su.⁸ A small contamination of the single gauze due to the accumulation of irrelevant materials on it may induce a high value of f , as pointed out by Su.⁸ In the present work, care has been taken to use a filter consisting of six layers of screen of 250 mesh per inch between the upstream gauze holder and conduit. The filter is considered to be able to effectively reduce such a contamination. The results are therefore more

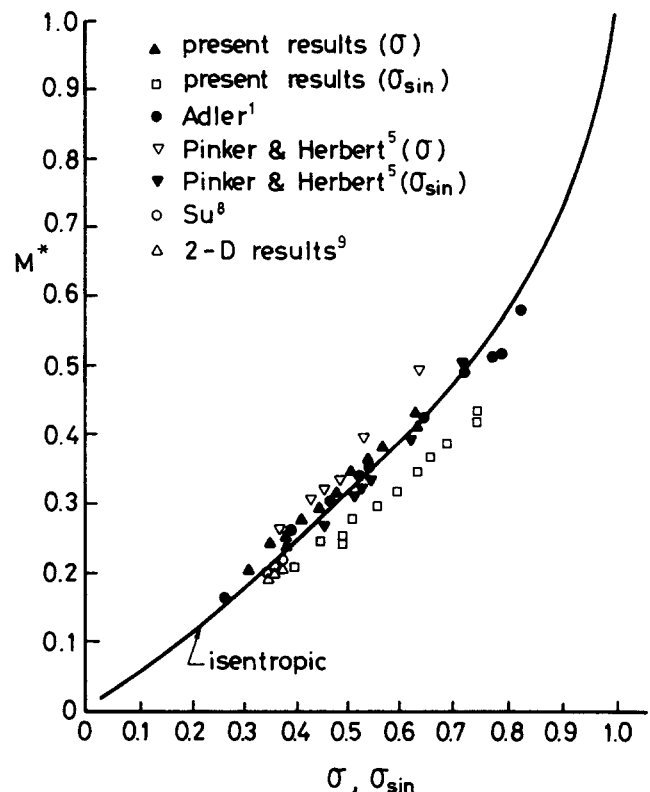


Figure 3 M^* versus σ and σ_{sin}

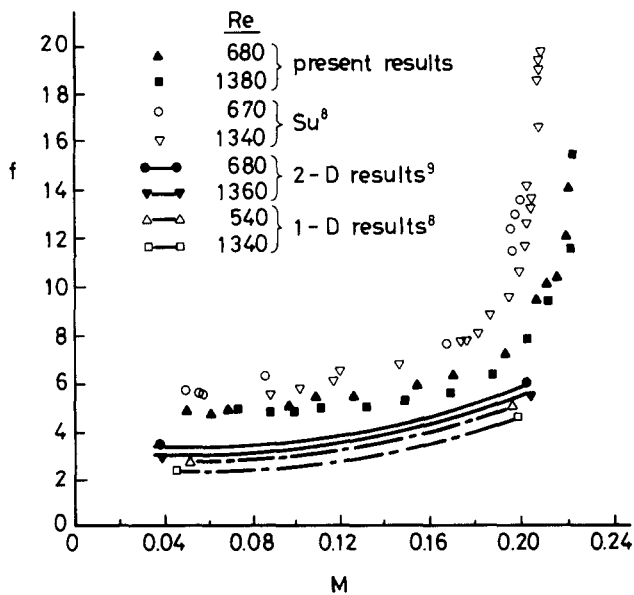


Figure 4 f versus M for $\sigma = 0.38$

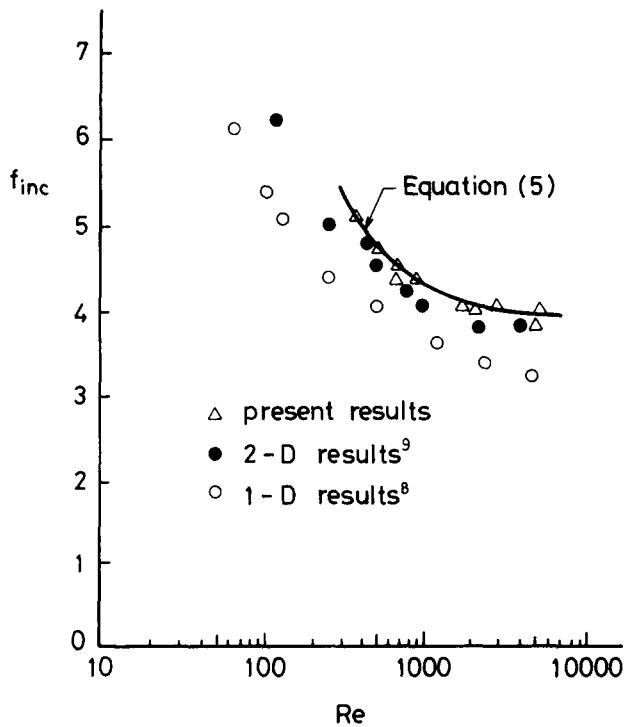


Figure 5 f_{inc} versus Re

reliable. On the other hand, the values of f of the present experimental work are higher than those obtained by both simulations involving a one-dimensional (1-D) and two-dimensional (2-D) core in the flow through single gauzes. Since the flow through gauzes is very complicated due to the weaving of the wire composing them, the present test results are therefore more trustworthy.

Effect of the Reynolds number

The evaluation of f using Equation 4 requires knowing f_{inc} beforehand. Figure 5 shows the effect of Re on f_{inc} . Based on

the present test results, the empirical expression for f_{inc} is

$$f_{inc} = f_{inc, Re=2000} \left(\frac{1 + 18.7\xi}{19.7\xi} \right) \tag{5}$$

where $f_{inc, Re=2000}$ is the incompressible pressure loss coefficient, f_{inc} , at $Re=2000$ and $\xi = Re/2000$. Equation 5 is also similar to those suggested by the above-mentioned earlier works. However, some difference exists, as can be seen from Figure 5: the values of f_{inc} of the present work are consistently higher than both results of flow simulations. It seems that the results of the 2-D model are closer to the test results than those of the 1-D model. The present test work is therefore a justification of the simulation of the 2-D model, even though the agreement between measured and simulated results is not very satisfactory.

Effect of the open area ratio

Although Figure 5 is plotted for gauze C ($\sigma = 0.38$), Equation 5 applies to other values of σ . Now $f_{inc, Re=2000}$ must be determined before using Equation 5. Figure 6 shows the variation of $f_{inc, Re=2000}$ with σ . Based on the data shown in Figure 6, an empirical expression for $f_{inc, Re=2000}$ is derived as

$$\log_{10} f_{inc, Re=2000} = -2.31\sigma + 1.46 \tag{6}$$

The curves drawn with Equation 6 and the empirical equation based on the 1-D model⁸ intersect at about $\sigma = 0.33$, as shown in Figure 6. At higher σ , the values of $f_{inc, Re=2000}$ of the present results are consistently higher. The 2-D flow model also demonstrates higher $f_{inc, Re=2000}$ than the 1-D model. Although the range of σ of the 2-D simulation is very narrow ($0.36 \leq \sigma \leq 0.38$), its results seem to support the present work. Figure 6 also shows the results of Adler¹ and Pinker and Herbert,⁵ which are for reference only, since the value of Re in their works is not known.

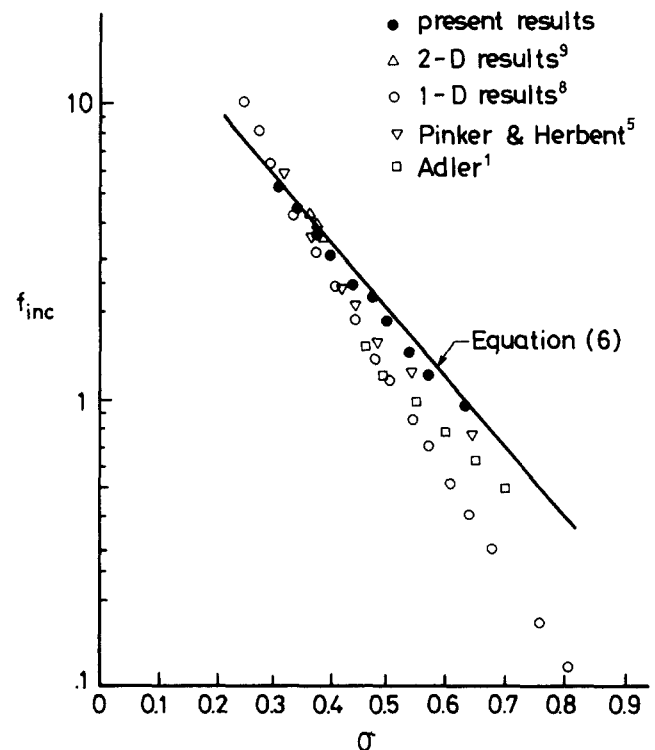


Figure 6 f_{inc} versus σ for $Re = 2000$

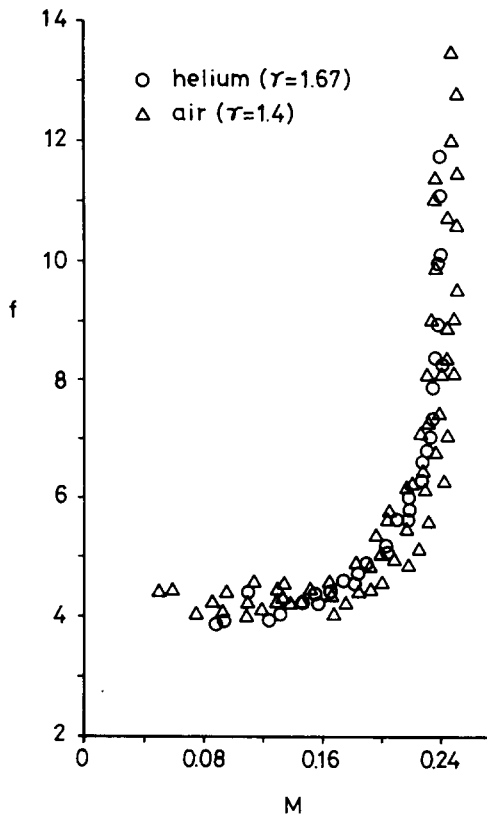


Figure 7 f versus γ

Effect of the specific heat ratio

In the simulation of the flow through single gauzes, the 1-D and 2-D models^{6,7} both indicate that the momentum thickness of the boundary layer on the wire surface is a function of M , Re , σ , and γ . Pressure loss characteristics are therefore expected to be affected by variation of γ . However, the effect of γ on f is negligibly small, as can be seen from Figure 7, in which f is plotted against M for two values of γ , i.e., 1.4 and 1.67 for air and helium, respectively. The results of the above-mentioned simulations also show this tendency. In addition, the experimental investigation by Su⁸ on packed gauzes with air, helium, and argon as the test fluids also supports this observation. The suspicion that different fluids might have different pressure loss characteristics due to γ is therefore removed.

However, $\Delta P/P_{up}$, a practical parameter that can be measured easily, is affected by the variation of γ . Figure 8 shows that for given M , Re , and σ , $\Delta P/P_{up}$ of helium ($\gamma=1.67$) is higher than that of air ($\gamma=1.4$). The difference is introduced by the ratio between the definitions of f and $\Delta P/P_{up}$, namely,

$$\frac{\Delta P/P_{up}}{f} = \frac{\Delta P/P_{up}}{\Delta P/(\rho u^2/2)_{up}} = \frac{1}{2}\gamma M^2 \tag{7}$$

Equation 7 shows that for a given γ , $(\Delta P/P_{up})/f$ is not constant but varies with M^2 . Therefore, the difference in $\Delta P/P_{up}$ for different γ increases with M , and the difference is small at low M , as shown in Figure 8.

It is clear, then, that f is a function of M , Re , and σ . A 3-D diagram showing pressure loss characteristics may be desired. Figure 9 shows the variation of f with M and Re for $\sigma=0.48$ (gauze F). Since the surface shown is plotted with experimental results, some ripples appear. To be practical, the 3-D diagram can be plotted with the empirical expressions discussed above,

i.e., Equations 4, 5, and 6. These expressions can be combined into a single equation as

$$f = 10^{(-2.31\sigma + 1.46)} \left(\frac{1 + 18.7\xi}{19.7\xi} \right) \left(\frac{M^*}{M^* - M} \right)^{0.16} \tag{8}$$

Diagrams showing the variation of f with two of the three governing factors, namely, M , Re , and σ , for a given value of the other factor can then be plotted with Equation 8. The results

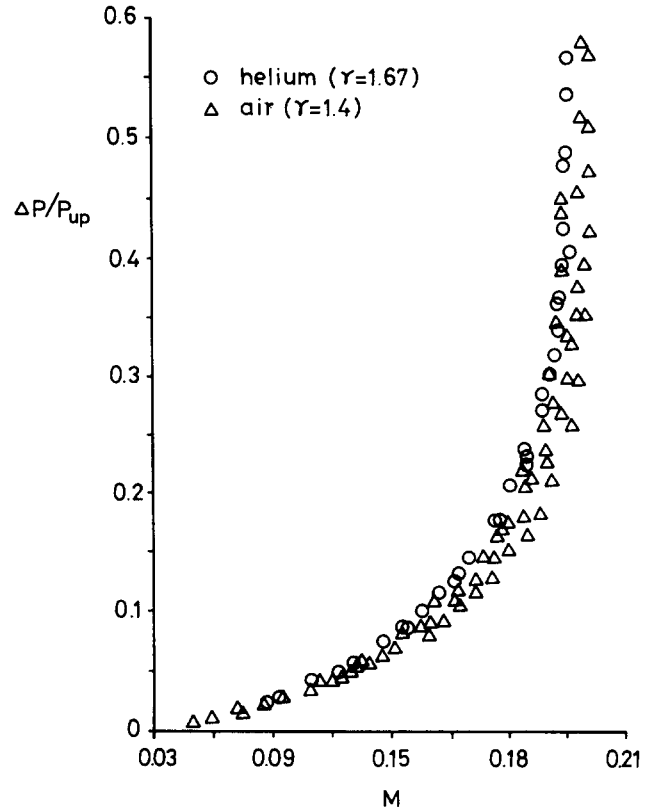


Figure 8 $\Delta P/P_{up}$ versus γ

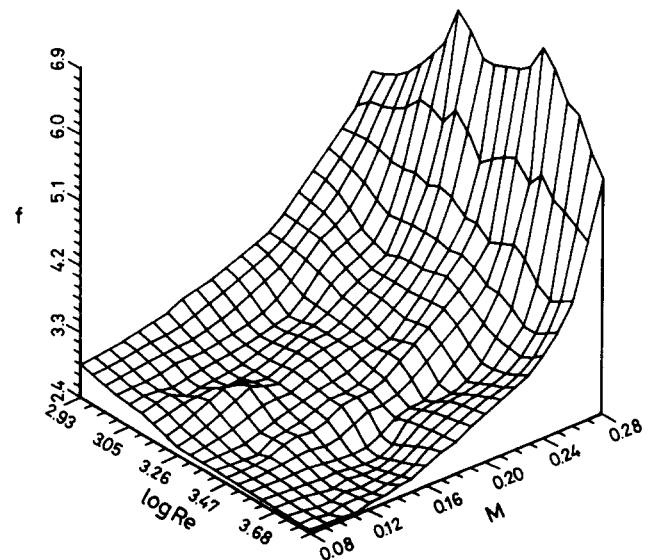


Figure 9 Three-dimensional diagram showing measured f versus M and Re for $\sigma=0.48$

will have the shape shown in Figure 9. (Note that Figure 9 is plotted with experimental data and thus appears to have some ripples.)

Conclusions

The pressure loss characteristics of the flow through single gauzes were investigated experimentally. The resultant data were compared with those obtained with the simulation of the flow modeled as a core outside a boundary layer developed along the surface of the wire composing the gauze. The following conclusions are drawn from this study:

1. The pressure loss coefficient, f , is a function of M , Re , and σ . Although the specific heat ratio, γ , may also be a governing factor, as indicated by flow simulations, the effect of γ on f is negligible. However, the ratio between the pressure drop across single gauzes and the upstream pressure can be affected by γ .
2. Depending on the upstream Mach number, choking may occur within the aperture of the gauze.
3. Before choking occurs, f increases with M . The increase is sharp at choking.
4. For the flow in the incompressible regime, f increases with decreasing Re .
5. Increasing σ has the effect of decreasing f .
6. The variation of f with M , Re , and σ can be obtained through an empirical equation, i.e. Equation 8.

Acknowledgments

The authors would like to thank the National Science Council

of the Republic of China for financial support of this work under contract NSC77-0401-E002-21.

References

- 1 Adler, A. A. Variation with Mach number of static and total pressures through various screens. *NACA Wartime Report*, No. L5f28, 1946
- 2 Annand, W. J. D. The resistance to air flow of wire gauzes. *J. R. Aero. Sci.*, 1953, **57**, 141–146
- 3 Wieghardt, K. E. G. On the resistance of screens. *Aero. Q.*, 1953, **4**, 186–192
- 4 Cornell, W. G. Losses in flow normal to plane screens. *Trans. A.S.M.E.*, 1958, **80**, 791–799
- 5 Pinker, R. A. and Herbert, M. V. Pressure loss associated with compressible flow through square-mesh wire gauzes. *J. Mech. Eng. Sci.*, 1967, **9**, 11–23
- 6 Roach, P. E. The generation of nearly isotropic turbulence downstream of streamwise tube bundles. *Int. J. Heat Fluid Flow*, 1986, **7**(2), 117–125
- 7 Roach, P. E. The generation of nearly isotropic turbulence by means of grids. *Int. J. Heat Fluid Flow*, 1987, **8**(2), 82–92
- 8 Su, C.-C. *An Enquiry into the Mechanism of the Pressure Drop in the Regenerator of the Stirling Cycle Machine*. Ph.D. Thesis, Engineering Department, Cambridge University, Cambridge, England, 1986
- 9 Su, C.-C., Hsieh, S.-S., and Chiu, M.-C. A simulation of flow-through wire gauzes. *Proc. 17th IASTED Int. Symp.*, Lugano, Switzerland, 1989, 234–237
- 10 Huang, C.-C. *Experimental Studies of the Pressure Drop of the Flow through Wire Gauzes used in the Regenerator of the Stirling Cycle Machine*. Masters Thesis, Mechanical Engineering Department, National Taiwan University, 1989
- 11 Loehrke, R. I. and Nagib, H. M. Control of free-stream turbulence by means of honeycombs: a balance between suppression and generation. *Trans. A.S.M.E. J. Fluids Eng.*, 1976, **98**, 342–353